Development of a Random Loading Test Bench for UD E-Glass/Resin Rotating Shafts with Integrated Monitoring of Failure Prediction

C.I. Basson[1*], G. Bright[1], J. Padayachee[1] & S. Adali[1]

ARTICLE INFO

Article details
Submitted by authors 9 Jan 2025
Accepted for publication 25 Mar 2025
Available online 30 May 2025

Contact details
* Corresponding author
bassonc@ukzn.ac.za

Author affiliations
1 Discipline of Mechanical Engineering, University of KwaZulu-Natal, Durban, South Africa

ORCID® identifiers
C.I. Basson
https://orcid.org/0000-0003-0737-5529

G. Bright
https://orcid.org/0000-0003-4386-0329

J. Padayachee
https://orcid.org/0000-0003-0358-5289

S. Adali
https://orcid.org/0000-0003-1781-1531

DOI
http://dx.doi.org//10.7166/36-1-3174

ABSTRACT

Rotating machinery, particularly shafts, is prone to failure owing to cyclic loading, bending stresses, and vibrational oscillations. To enhance their longevity and minimise failures, a predictive maintenance strategy is proposed that integrates Hotelling's T-squared clustering. Clustering identifies key operational profiles, while embedded sensors gather vibration, temperature, and current data for feature extraction via principal component analysis. The results show that predictive monitoring identifies the remaining useful life of shafts by leveraging data-driven insights, emphasising material-specific characteristics for precise prediction of failure and improved reliability.

OPSOMMING

Roterende masjinerie, veral asse, is geneig om te faal as gevolg van sikliese laai, buigspannings en vibrasie-ossillasies. Om hul lewensduur te verbeter en mislukkings te verminder, geintegreerde voorspellende instandhouding strategie met Hotelling se T-squared-groepering word voor gestel. Groepering identifiseer sleutel operasionele profiele, terwyl ingebedde sensors vibrasie, temperatuur en huidige data versamel vir kenmerk-onttrekking via hoofkomponent-analise. Die resultate toon dat voorspellende monitering die oorblywende nuttige lewensduur van asse identifiseer deur gebruik te maak van data-gedrewe insigte, hoofsaaklik materiaal-spesifieke eienskappe vir presiese falingsvoorspelling en verbeterde betroubaarheid.

1. INTRODUCTION

1.1. Development of test bench for rotating machines that incorporates monitoring of failure prediction

Rotating machines can fail owing to high-stress loadings and vibrational oscillations while operating continuously. Shafts are especially vulnerable to deflection and bending loads. The actuator transmits torque and speed to the working device via a rotating shaft. The shaft's performance is influenced by its stiffness. The stiffness and mass have an impact on the vibrational output [1]. Heat transmission, vibration, and chatter all affect the shaft's operational performance [2]. Because of cyclic loading-induced damage to component materials and their declining health, rotating shafts gradually lose their working life. Monitoring shaft health diagnostics and failure prediction is essential to extending the shaft's operational lifespan and reducing the likelihood of catastrophic machinery damage [3]. A conceptual predictive maintenance system for rotating machines is shown in Figure 1.

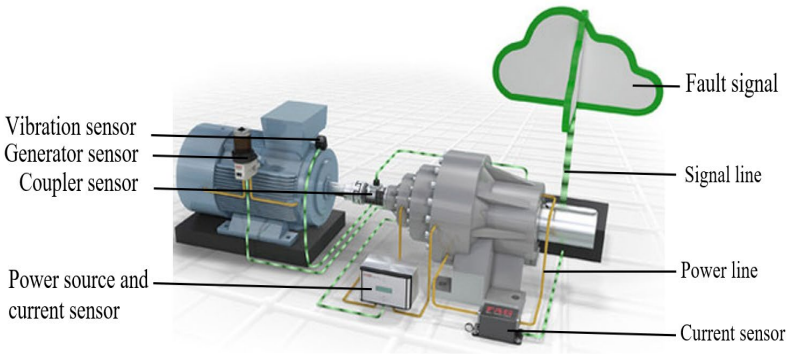

Figure 1: Conceptual rotating machine maintenance system [2]

Patterns hidden in the failure of rotating machinery that is constructed of composite materials enable failure prediction. The workflow of the proposed predictive monitoring system with predictive analytics consists of six components: data collection, data processing, pattern identification, prediction generation, prediction response and response measurement (see Figure 2). Initial sensor data collection and transmission to a database for storage constitute the process's first stage. Data transformation and reduction strategies are used to process the data in order to extract key features [4]. An AI-supervised algorithm looks for a pattern in the data, based on its attributes. The discovered pattern is validated in order to generate predictions. Predictions are produced, and the model is optimised. In the next step, a hardware feedback change is implemented using actuator control in response to the forecasts. The mechanical response of the machinery is influenced and measured by a control algorithm. The response is sent to the data collection process after being quantified. The procedure is repeated during the machinery's operational life. In this study, actuator control for response was only mentioned as an operational consideration and was not investigated [5].

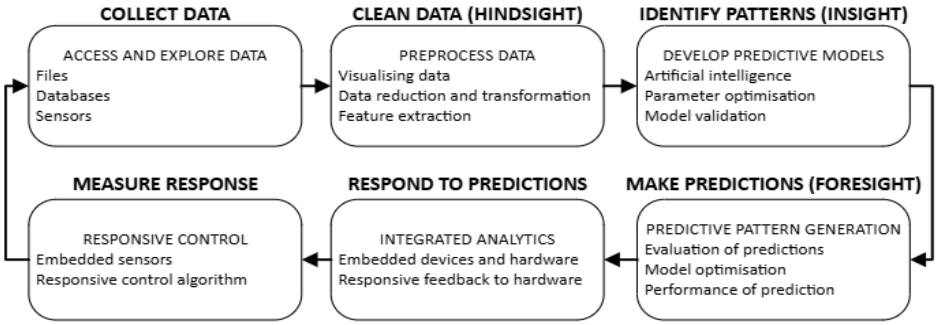

Figure 2: Conceptual rotating machine maintenance [5]

The aim was to design a random loading test bench for composite shafts that replicates unpredictable real-world stress conditions while integrating failure prediction models. Composite materials make it problematic to estimate their general remaining useful life (RUL) under arbitrary bending loads because of their nonlinear fatigue behaviour. To improve the accuracy of failure forecasting, the system must link sensor data with predictive analytics and capture the evolution of stochastic stress. Through integrating statistical models and machine learning techniques for predictive maintenance, the study seeks to validate the dependability of composite shafts under random loading.

1.2. Research's contribution

This study advances the field of predictive maintenance (PdM) for rotating composite shafts by combining multivariate anomaly detection and fatigue life prediction methods. The study offers a novel parametrisation method for predicting the remaining useful life (RUL) of composite shafts under random bending loads using Hotelling's T-squared clustering. In order to address the distinct failure characteristics of composite materials, especially under variable loading conditions, the research framework integrates diagnostic and experimental procedures.

A custom random load spectrum was developed for use in an R.R. Moore test setup [6], providing valuable insights into the fatigue behaviour of composite-based rotating machinery. The research methodology was tested against real-time operational data to assess its accuracy in forecasting failures. It offers practical implications for enhancing reliability and operational efficiency in industries that rely on composite rotating components.

The following are the key scientific contributions of the paper:

- Development of a novel predictive maintenance strategy by integrating Hotelling's T-squared clustering [7], tailored for composite shafts under random loads.
- Design and implementation of experimental data for pultruded UD E-glass shafts, contributing to a deeper understanding of composite failure behaviour under rotating conditions.

2. LITERATURE REVIEW

2.1. Predictive maintenance strategy

The PdM philosophy is defined as using the actual and current state of equipment to improve and optimise a plant's operation. The condition monitoring (CM) of equipment and parts that rely on the current condition of the equipment is known as condition-driven preventive maintenance or CDPM. Figure 3 illustrates how predictive models use data-driven and sensor feedback to forecast the maintenance threshold for machinery [8]. PdM models predict part-life based on a range of machine-health indicators, system efficiencies, and mechanical conditions instead of average-life statistics [9]. CM uses instruments and sensory systems to monitor symptoms of health and failure, such as vibration, temperature, and acoustic emissions.

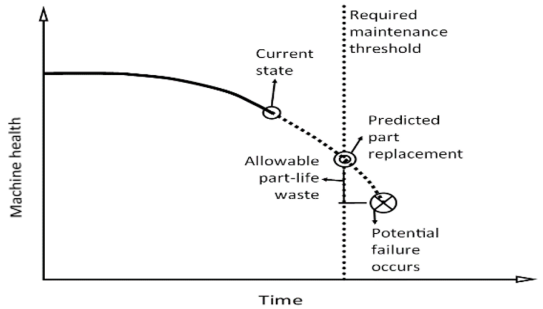

Figure 3: Predictive maintenance management strategy [9]

2.2. Evolution of composite damage

There are mainly two ways in which composite damage manifests. Unlike isotropic materials, which usually have a single isolated crack that controls the progression of damage, composite materials are characterised by diffused multiple cracks during the early and middle stages of the material's lifecycle [10]. Matrix cracks frequently follow the fibre's path, causing directional damage to composite materials in laminates. This leads to the classification of different types of diffuse damage according to their orientation in the material [11]. Observations of the functional endurance of composites with cracks indicate that over 50% of their damage occurs in the first 20% of their lifespan [12]. Figure 4 illustrates the evolution of the composites' damage. Traditionally, fatigue is analysed through linear damage models by determining the proportion of damage for each stress cycle. The linear damage rule (LDR) makes the same assumptions as the Palmgren-Miner rule: that work is continuously absorbed for each cycle, and that a specific amount of work is absorbed in failure. A modified Marco-Starkey model is a nonlinear load-dependent theory of damage accumulation that was proposed by Ali *et al.* [13]. A particular instance of the Marco-Starkey theory in which $C_i = 1$ is the Palmgren-Miner rule:

$$D = \sum \left(\frac{n_i}{N_i}\right)^{C_i} \tag{1}$$

where n_i is the number of stress cycles at stress level σ_i experienced by the component, and the number of cycles that would cause failure at stress level σ_i is expressed by N_i.

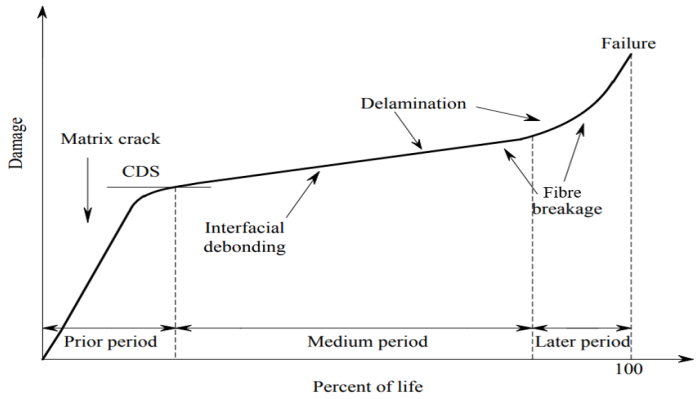

Figure 4: Evolution of damage in composites [11]

2.3. R.R. Moore fatigue test bench method with active feedback and fluctuating loadings

The R.R. Moore fatigue test method is commonly used to evaluate material fatigue under rotating bending conditions. However, a key limitation is its application of constant loading, which prevents the generation of variable loading amplitudes. This makes it less suitable for analysing random loading fatigue in rotating shafts [14]. A variable amplitude loading fatigue test bench with an actuator and load cell to provide active feedback to the system was designed by [15]. The active feedback controls the loading force that is applied to the rotating specimen (Figure 5). The purpose of the test bench was to examine the rotating beam's fatigue properties under high rotations and random loading.

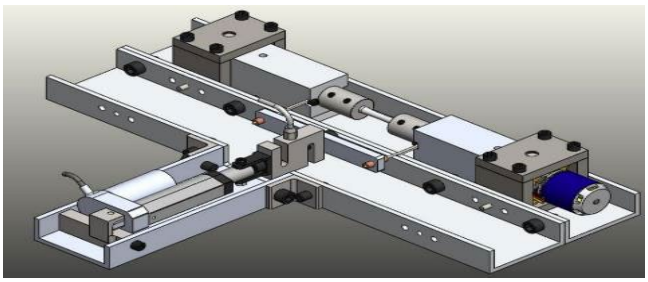

Figure 5: Variable amplitude fatigue testing machine for rotating shafts [15]

3. PROPOSED METHODOLOGY AND DESIGN

3.1. Methodology for structural prognostic testing

The primary objective of the proposed methodology was to develop a PdM strategy that identified operational profiles using Hotelling's T-squared clustering. In addition, the method was developed to analyse the parametrisation of the RUL curve using Weibull parameters for future work. This methodology has several crucial steps (see Figure 6). The first step in extracting material properties is tensile and flexural testing. Data on fatigue life is then obtained through simulations using finite element analysis (FEA). In addition, a rotating fatigue test bench with a variable load is used to collect relevant data parameters. To find different operational profiles and to detect RUL, this data is subjected to Hotelling's T-squared clustering. These clustering results are then incorporated into a Weibull-modified linear damage model to enhance the estimating of fatigue life. The strategy also calls for the creation of decision rules and maintenance thresholds that are based on this integrated approach. Finally, the performance of the developed PdM strategy is evaluated and confirmed to be effective. This paper focuses only on the performance of the machine learning component of the test bench (steps 3 and 4 in Figure 6). The Weibull-modified model and the origin of fatigue data are mentioned to explain the context of this study, but they were not the focus of this paper, which covers the development of the test bench in step 3 and the output results in step 4 in the methodology that is proposed below.

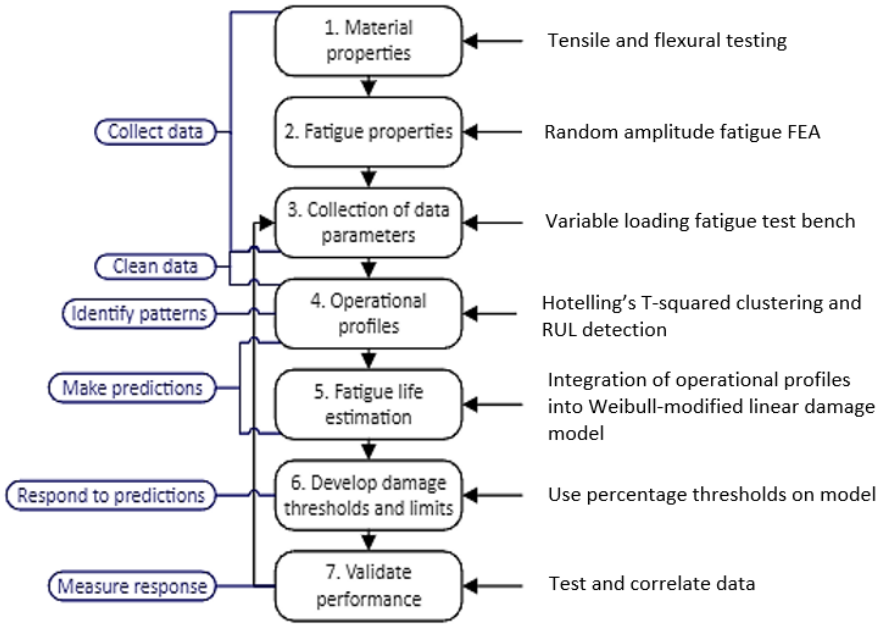

Figure 6: Proposed methodology for structural prognostic testing

The programme's flow is shown in Figure 7, which includes the machine learning (ML) algorithm using principal component analysis (PCA) and Hotelling's T-squared clustering [16], [17]. Importing the necessary libraries for data processing initialises the programme. The data acquisition system provides the experimental data, which is then imported into the Python application. The raw data is stored and visually plotted. Outliers and redundant data are removed from the recorded data, and each sensor data set is given a feature. Standardised data is used for PCA calculations. The data is subjected to PCA, and a two-dimensional plot is produced to visualise the data manipulation.

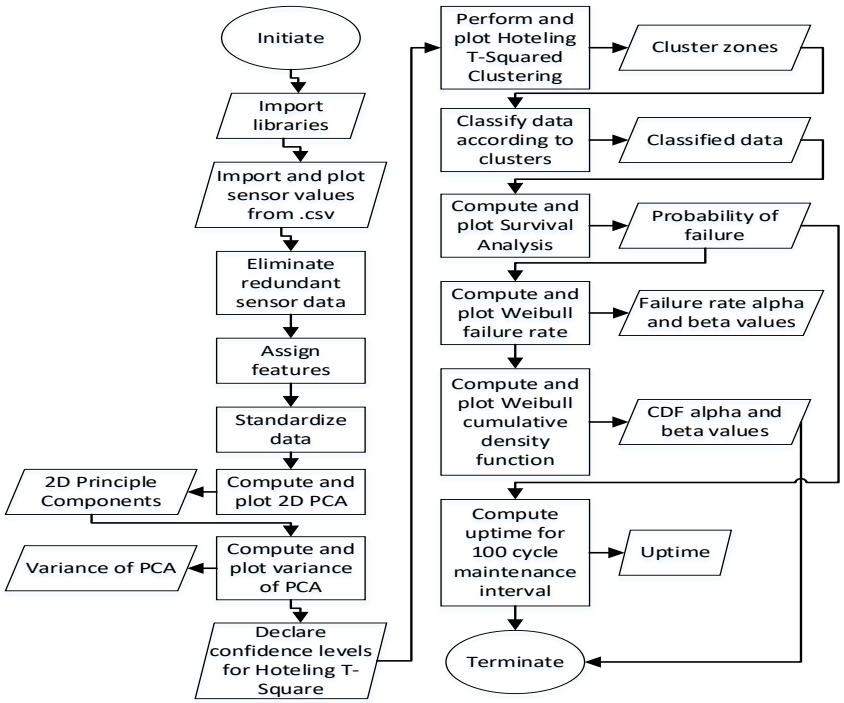

Figure 7: Programme flow chart of the prognostic model

3.2. Design for random loading

The principles of shaft bending fatigue were used to design a test bench for rotating machinery. The shaft undergoes pure bending when it rotates. A mechatronic architecture design can be used to explain the design and development of the rotating test bench. The mechatronics framework consists of embedded software and mechanical components, as shown in Figure 8. The fatigue bench has two main subsystems: the prognostic system and the load spectrum application. The load spectrum application applies a random load to a rotating shaft through pure bending moments. The random spectrum is produced by fluctuating the maximum load to be used, which is determined at random intervals by a microcontroller. The microcontroller receives the output steps via voltage signals. The linear drive applies bending loads to the shaft after it has received the output steps from the motor controller. Forces generate the bending loads owing to linear drive displacements. The prognostic system consists of a motor and corresponding mechanical component, as well as embedded sensors on the bearings of the rotating shaft. Based on user-input pre-set RPM values, the microcontroller in the fatigue test bench rotates the composite shaft. The sensory system logs the temperature, current, and vibration data that come from the rotation and load spectrum reaction displacements when a shaft fails. The information is then entered into a Python application for additional processing and a prediction of shaft failure.

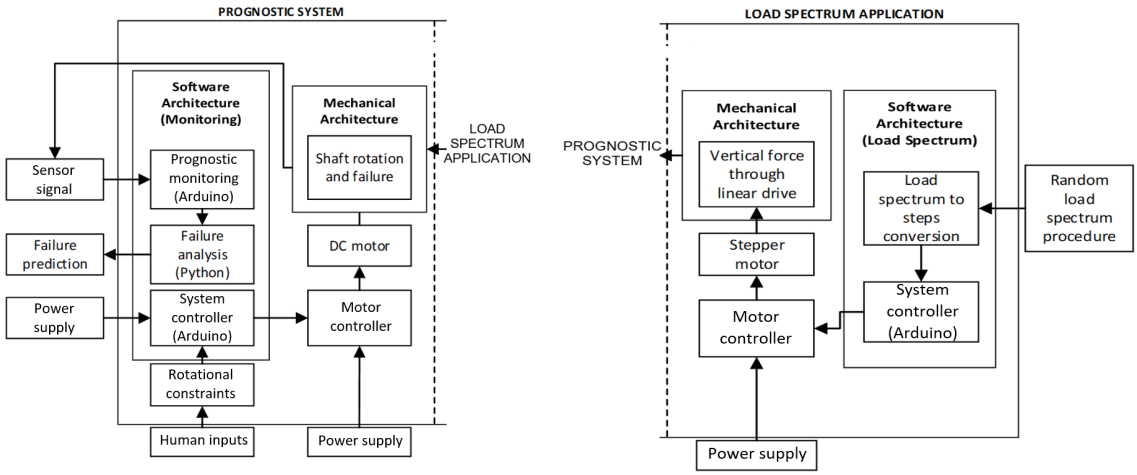

Figure 8: Load spectrum application and prognostic system design of the test bench

A test bench was needed to acquire the operational data for prognostics on a rotating shaft, A four-point bending load test bench method was recommended, as seen in Figure 9. This design was an enhanced version of the test bench developed by Basson *et al.* [18]. The point loads were applied at bearings B and C. The shaft was limited at bearings A and D. Temperature, current, and vibration data were recorded using accelerometers on bearings B and C. Current data from the motor was acquired by connecting a current sensor in series with the power source line. The rotational speed was measured at sensors R1 and R2 along the shaft in order to determine total shaft failure. A linear actuator was used to apply the random cyclic loading with respect to the vertical point loads at bearings B and C. The shaft experienced pure bending because of the vertical forces acting on the shaft.

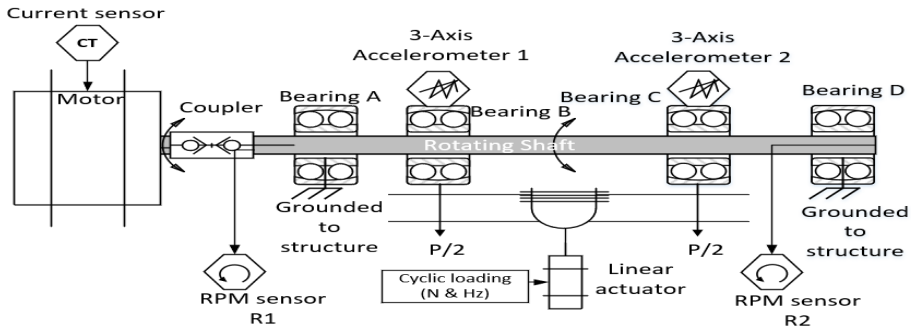

Figure 9: Conceptual design of test bench

3.3. Complete assembly

The test bench frame was intended to provide high stiffness and rigidity so that it could support heavy loads, and so it was built with square tubing (3). The test bench was equipped with a direct current (DC) motor (11) for high rotation speeds, a linear drive (1), and a stepper motor for load cycle control. Guide rods (2) could restrict the vertical displacement of the shafts (5) and (9), which were controlled by a spherical bearing (8). The shaft was mounted to the frame using a pillow bearing (4), and the composite shaft (7) was prevented from slipping by a collet fastening system (6). In addition, an aluminium angle bar (10) was used to mount the sensor. The design of the rotating test bench is shown in Figure 10.

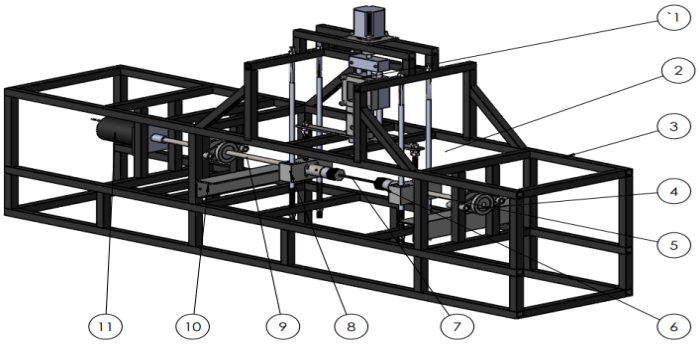

Figure 10: Computer-aided model of test bench assembly

3.3.1. Specimen shaft assembly

The specimen is a 6.9 mm diameter solid rod composed of pultruded vinyl ester resin and unidirectional E-glass. Table 1 lists the specimen's attributes. The volume fraction ratio of the fibre and resin properties was used to compute the theoretical stress.

Table 1: Composite shaft material properties

Material property	Symbol	Value
E-glass tensile strength	$\sigma_{UTS_{fibre}}$	$1970\ MPa$
Fibre density	ρ_{fibre}	$2.41\ \frac{kg}{m^3}$
Vinyl ester tensile strength	σ_{resin}	$79\ MPa$
Vinyl ester density	ρ_{resin}	$1.07\ \frac{kg}{m^3}$
Fibre mass percentage	MF	85%
Fibre volume percentage	VF	67%
Fibre/resin theoretical strength	σ_{UTS}	$1346\ MPa$
Radius	r_o	$6.90\ mm$
Second moment of inertia	I	$1.1786e-10\ m^4$

To withstand the same bending and rotational loading as the entire shaft assembly, the specimen needed to be firmly attached to a modified shaft. The test conditions for the specimen were comparable to those that would be applied to a rotating shaft. Figure 11 shows the specimen shaft assembly. Two collet assemblies (2 and 5) hold the fibreglass and resin shaft specimen (1) in place. The collet assembly is attached on both sides to a solid coupler (3). The one part of the stainless steel drive shaft (4) connects to the motor assembly via a bearing, while the other drive shaft (6) is free and is mounted to a bearing.

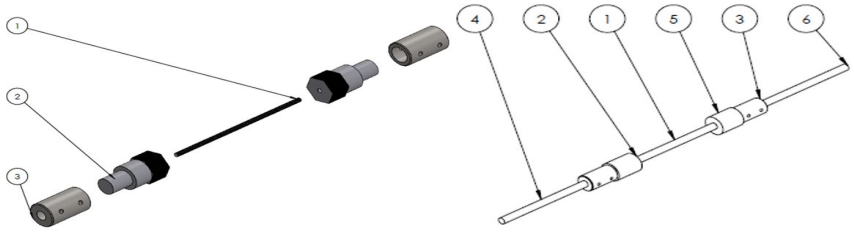

Figure 11: Specimen shaft assembly

3.3.2. High-speed rotational assembly

To rotate the specimen assembly for testing under four-point bending, a high-speed DC motor is needed. A flexible coupler (3) connects the high-speed DC motor (1) to the stainless-steel shaft (4). A mounting plate is used to attach the rotating assembly to the spaceframe (2). Figure 12 shows the actuation system assembly.

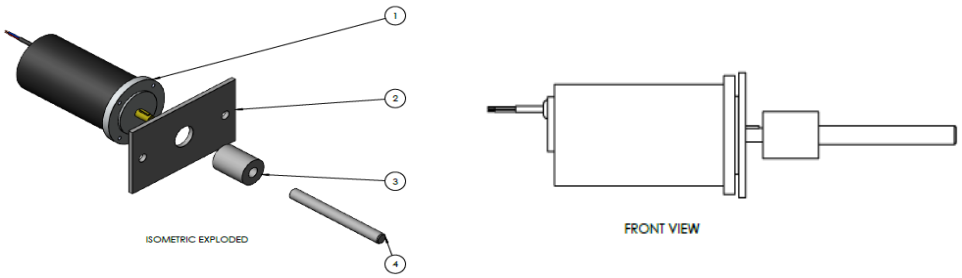

Figure 12: Computer-aided model of high-speed rotational actuation assembly

3.3.3. Random loading assembly

The four-point bending load is applied to the shaft via the linear slide by the random loading system. A stepper motor provides rotational movement to a lead screw linear drive, which carries out the linear actuation. The linear slider and stepper motor are attached to the spaceframe. The linear slider's spherical bearings, which are attached to the specimen assembly's drive shaft, enable pitch, yaw, and roll, eliminating restive moments in those directions. Figure 13 shows the random loading assembly.

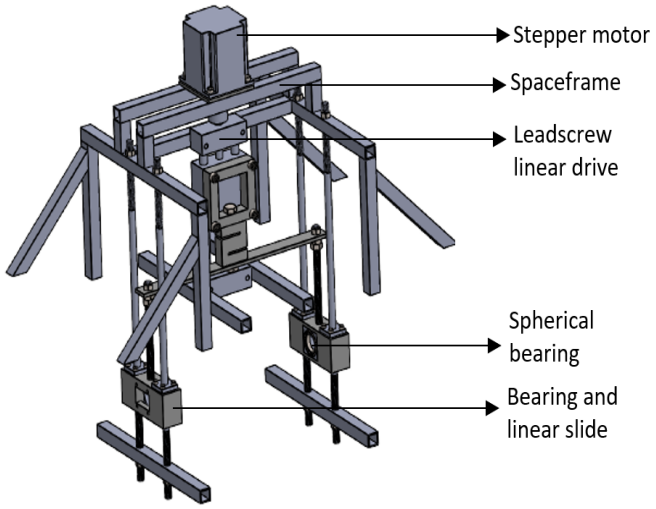

Figure 13: Computer-aided model of random loading actuation assembly

3.4. Test bench specifications, calibration, and modification

Tightening the ends of the specimen on to a conical collet chucking mechanism allowed it to be placed on to the rotating fatigue test bench. The shaft assembly was connected to a 12-volt DC motor for transmission. The operating speed was set to 1500 RPM when under load. Four-point bending was used to load the shaft assembly. The bending moment was created by applying displacement to the shaft assembly with a linear drive and stepper motor. The rotational speeds of the stepper motor were 500 RPM and 1.8° per step. Steps in the random displacement spectrum ranged from 90 to 3600. At various speed rates, a loading ratio of R = -0.8 was used owing to the motor's restricted speed. As shown in Figure 14, a maximum displacement of 27 mm was measured using a dial gauge. Each specimen was tested for 30 minutes at a sampling rate of 58 ms (17.24 Hz) under the conditions mentioned above. The cycle counting range of the Arduino Mega microcontroller was limited to 32767 and -32768 because of its 16-bit memory limit. The operational conditions are given in Table 25.

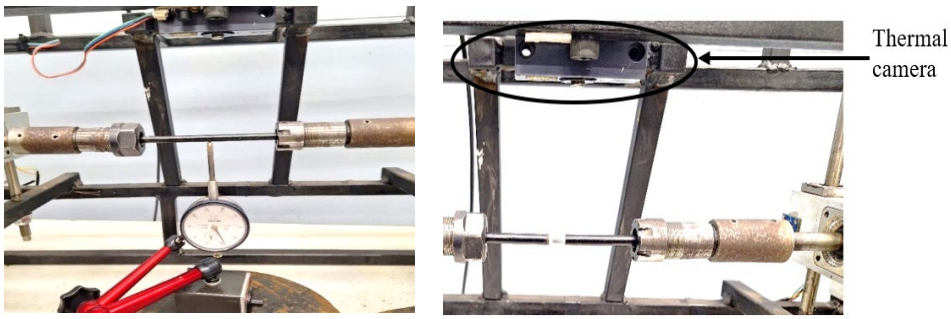

Figure 14: Deflection calibration and placement of thermal camera

Using the experimental setup, it was discovered that the shaft was constrained under cantilever loading conditions. The shaft was connected directly to the motor, and a double universal joint was required as a flexible coupler to replicate the reaction moment. The test bench modification is shown in Figure 15.

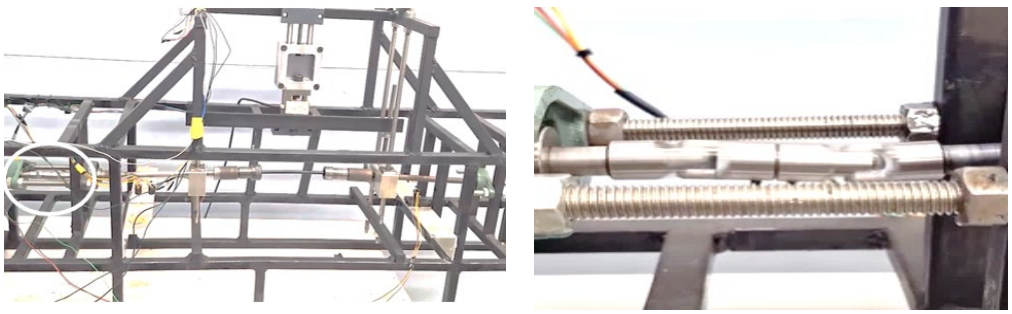

Figure 15: Test bench modification for four-point bending

Under bending stress, specimen E failed at 35580. Bending failure is indicated by splintering at the critical failure region (Figure 16). Specimen E was chosen as the more suitable specimen. Table 2 contains the specimens' failure results. The cycles to failure for specimen E were ascertained by averaging the five samples that failed under the loading conditions.

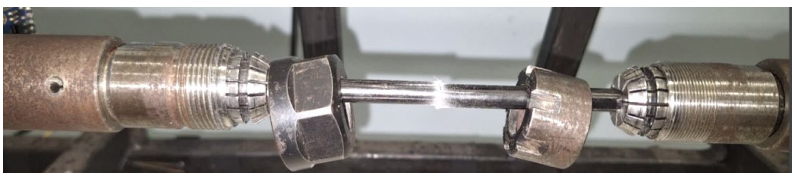

Figure 16: Specimen failure in collet assembly

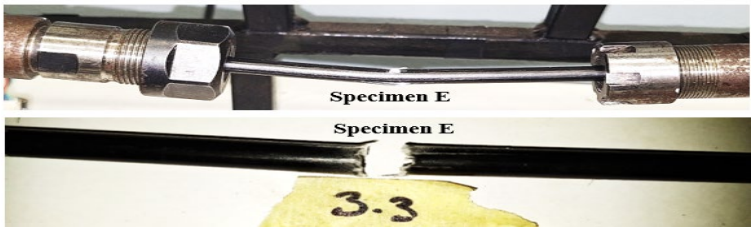

Figure 17: Specimen failure in collet assembly

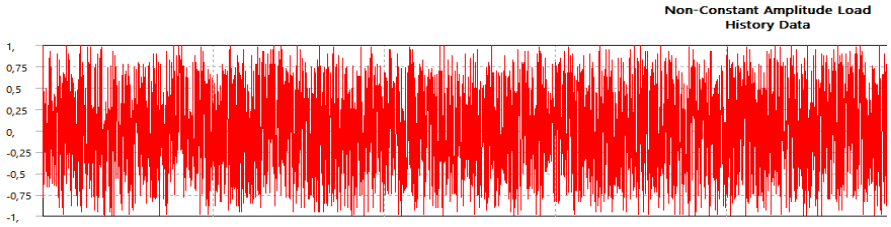

Figure 18: Random ordered load amplitude spectrum input for R = -0.8

Table 2: Specimen performance and testing results

Specimen	Failed (Yes/No)	Failure mode	Tested cycles
A	No	N/A	65535
B	No	Longitudinal cracking	65535
C	Yes	Shear failure	8807
D	Yes	Shear failure	1532
E	Yes	Bending failure	35580 (average)

4. EXPERIMENTAL RESULTS

4.1. Data preparation

To create a single dataset for processing, the raw data from Samples 1–5 of Specimen E was compiled. The raw data included all vibrational, temperature, and current data, as shown in Figures 19–23, and was pre-processed to reduce the impact of outliers and to smooth it out. The raw data was subjected to the following features: ambient temperature, object temperature, and current. The X, Y and Z directional accelerations were measured at bearing 1 and bearing 2. The z-score and moving average methods were applied.

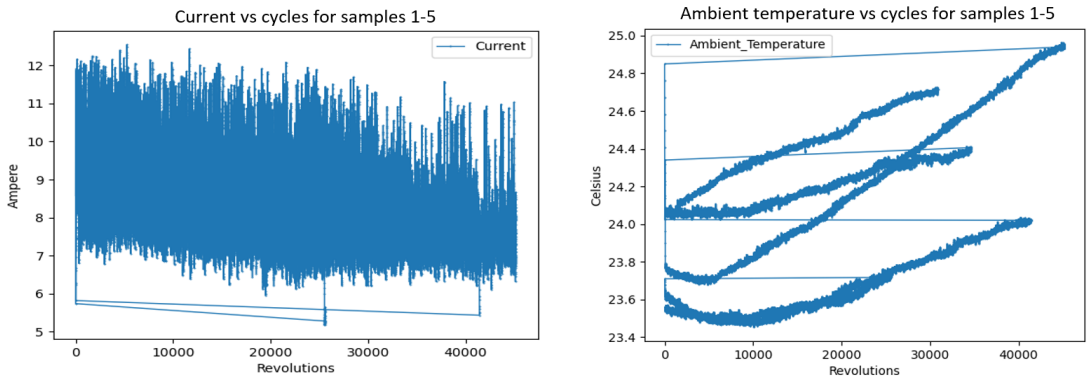

Figure 19: Processed raw data from sensors for samples 1-5 of specimen E (current and ambient temperature)

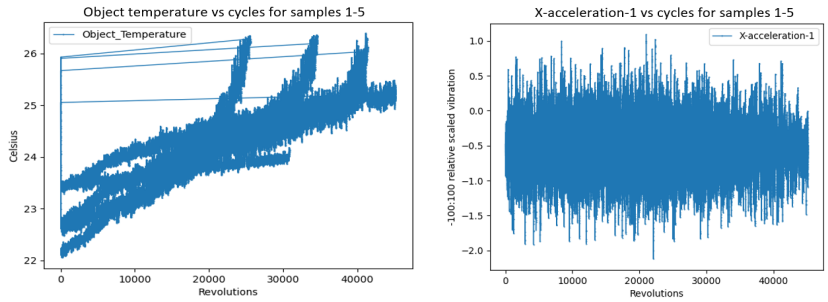

Figure 20: Processed raw data from sensors for samples 1-5 of specimen E (object temperature and x-acceleration sensor 1)

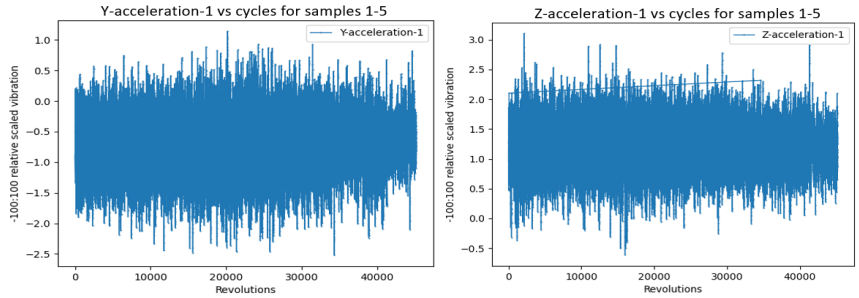

Figure 21: Processed raw data from sensors for samples 1-5 of specimen E (y-acceleration sensor one and z-acceleration sensor 1)

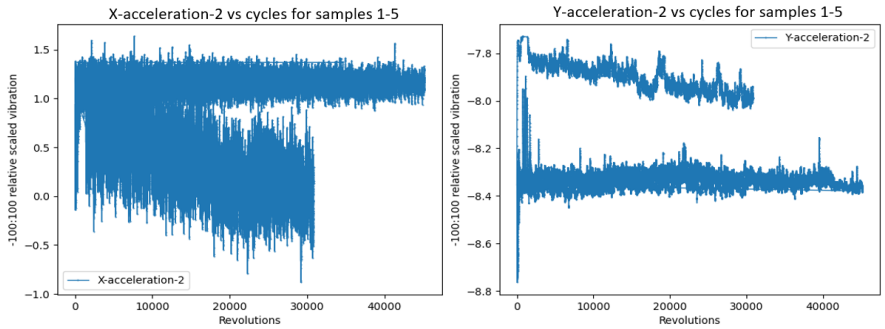

Figure 22: Processed raw data from sensors for samples 1-5 of specimen E (x-acceleration sensor two and y-acceleration sensor 2)

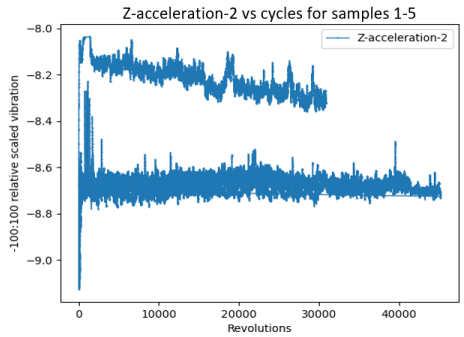

Figure 23: Processed raw data from sensors for samples 1-5 of specimen E (z-acceleration sensor 2)

As seen in Figure 24, the raw data was aggregated and subjected to a PCA, as described by [19]. To examine the overall variance of principal components 1 and 2, a cumulative variance bar graph was created. Figure

24 illustrates the total cumulative variance, which was determined to be 49%. Since 80% is required to explain the data adequately and to minimise data variance loss, the cumulative variance of the raw data had to be improved. To increase the cumulative variance, data features had to be deselected.

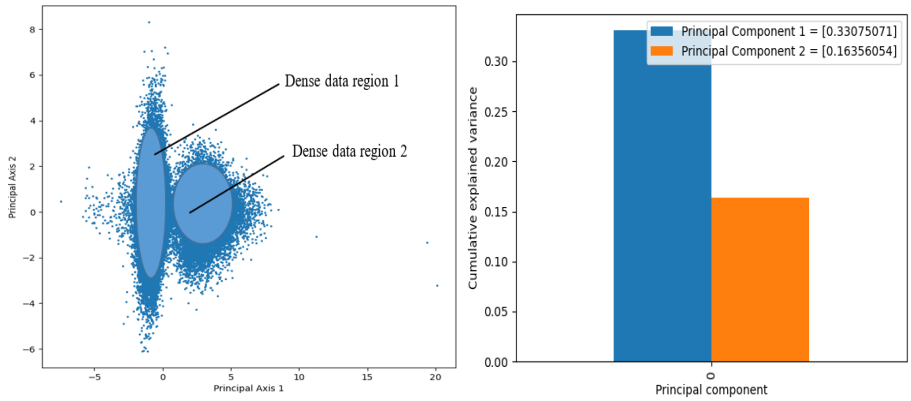

Figure 24: PCA for raw data, illustrating dense regions and cumulative variance of raw data

From the raw features, current and object temperature were determined to be critical features, and were classified as usable features when the cumulative variance was greater than 80%. As seen in Figure 25, a PCA was conducted after the data had been aggregated and, as shown, the calculated cumulative variance was 85.49%, which was above the 80% cut-off. Data migration from a densely populated area to the upper right of the graph reveals a visual pattern. The PCA clearly shows abnormal visual patterns for important features.

Initially, it was assumed that detecting vibrational changes from specific locations would yield useful information for forecasting. However, recognising patterns was difficult, as experimental analysis showed that the raw vibration data revealed erratic and non-linear patterns. Although linear relationships could be produced from vibration data using power spectral density analysis, this analysis was outside the purview of the study. Vibration data was thus eliminated as a component of the study.

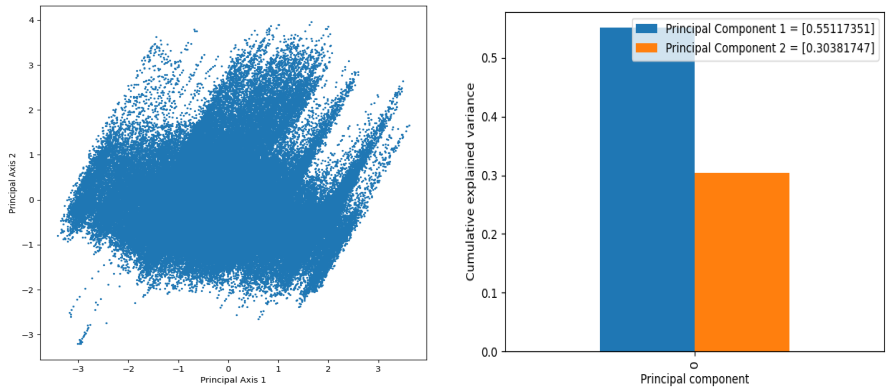

Figure 25: PCA of critical features and cumulative variance of critical features

The elliptical clustering of the Hotelling T-squared algorithm for the critical features was subjected to a survival analysis. The quantity of normal data that had not moved to other zones is counted in the RUL graphic. The characteristic curve of the deterioration plot of the important characteristics data is shown in Figure 26. At each occurrence, normal data migrates to a different zone, deducting from the overall fraction of runs. Figure 26 displays the total number of alerts divided by the total number of unique cycle counts, as well as the total number of warnings divided by the total number of unique cycle counts. The volume of warning and alarm data for particular failure cycles is shown in red and yellow. The area inside the green circle represents the usual operation data. The data points are classified into regions to each particular confidence level, and the sum of each region is plotted.

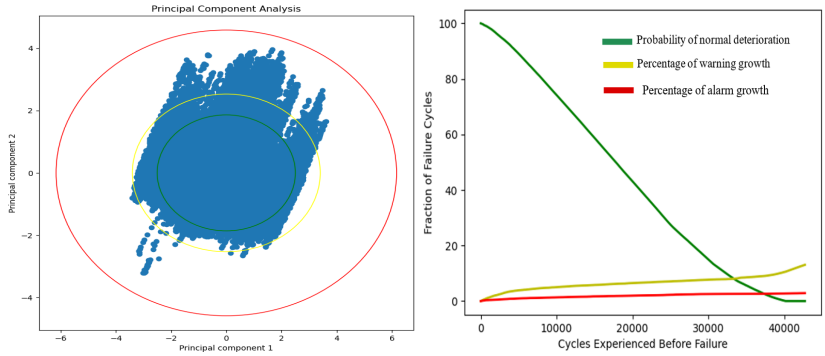

Figure 26: RUL and cumulative warning and alarm fractions concerning the sum of local unique counts

Critical features were extracted from the temperature and current data. After conducting the prediction analysis, a RUL was produced. The RUL was compared with the theoretical values and tabulated in Table 3. The theoretical damage values were extracted from [20]. The prediction model produced a reverse damage evolution curve that resembled the composite damage evolution curve. Further refinement and experimental work was required to achieve the reliability of the proposed model. The predicted maximum cycles of 44.25% was close to 50% of the damage, which was an improved performance compared with the theoretical fraction cycles of 20%.

Table 3: Performance of failure prediction

Criteria	Performance
Amount of damage	50%
RUL %	50%
Revolutions	17794
Fraction of max cycles	44.25%
Fraction of warning	47.48%
Theoretical fraction of max cycles	20%

5. CONCLUSIONS

The proposed PdM methodology effectively combines advanced statistical techniques with practical testing setups to address failure prediction problems in rotating shafts. Integrating Hotelling's T-squared clustering with the strategy provides robust insights into damage accumulation, operational profiles, and the estimation of fatigue life. The incorporation of collected real-time data and extracted critical features through PCA ensures that the model remains adaptive and reliable in diverse operational conditions. Furthermore, the exclusion of non-critical features, such as vibration data, underscores the importance of focusing on quantifiable and predictive metrics for machinery diagnostics.

The study highlights the importance of designing specialised test benches, such as the four-point bending configuration, to simulate real-world loading conditions and to capture accurate failure data. The emphasis on data pre-processing, including removing outliers and selecting features, enhances the model's predictive accuracy. The results from the survival analysis and RUL plotting validated the efficacy of the proposed approach, with insights showing significant potential for extending machinery's lifespan while minimising maintenance costs and downtime.

Future work could build on this foundation by integrating actuator control mechanisms for automated feedback systems and exploring advanced spectral analysis techniques for vibrational data. The algorithm allows for Weibull algorithm integration and for the generation of Weibull parameters to improve damage models. By refining the model further and expanding its application, this methodology should hold promise for updating predictive maintenance practices across different industries, thus ensuring higher reliability and operational efficiency in rotating machinery systems.

REFERENCES

[1] **Aralaguppi, R. H., Shashikumar, M. M., Siddesh, K. B. and Badhe, N. B.** 2018. Study on machine tool spindle shaft dynamics considering the effect of mass of two balancing discs. HPC CIRP High Speed Machining, Budapest.

[2] **Ringsell, S. F.** 2017. Why rotating machine maintenance is crucial in avoiding downtime. Process Engineering. [Online]. Available: https://processengineering.co.uk/article/2023520/why-rotating-machine-maintenance-is-crucial-in-avoiding-downtime [Accessed 14 September 2020].

[3] **Lin, T. R., Tan, A. C. C., Howard, I., Pan, J., Crosby, P. and Mathew, J.** 2011. Development of a diagnostic tool for condition monitoring of rotating machinery. In Proceedings of ICOMS Asset Management Conference, Gold Coast, Australia.

[4] **Lee, J., Chen, Y., Abuali, M. and Lapira, E.** 2009. A systematic approach for predictive maintenance service design: Methodology and applications. International Journal of Internet Manufacturing and Services, 2(1).

[5] **MathWorks.** 2020. Designing algorithms for condition monitoring and predictive maintenance. MathWorks. [Online]. Available: https://www.mathworks.com/help/predmaint/gs/designing-algorithms-for-condition-monitoring-and-predictive-maintenance.html [Accessed 28 September 2020].

[6] **Sepahpour, B.** 2014. A practical educational fatigue testing machine. In 121st ASEE Annual Conference & Exposition, Indianapolis.

[7] **Shaohui, M., Tuerhong, G., Wushouer, M. and Yibulayin, T.** 2022. PCA mix-based Hotelling's T^2 multivariate control charts for intrusion detection system, IET Information Security, 16(3), pp. 161–177.

[8] **Mobley, R. K.** 2002. An introduction to predictive maintenance: A volume in plant engineering, 2nd ed. Woburn: Butterworth-Heinemann.

[9] **Sirvio, K. M.** 2015. Intelligent systems in maintenance planning and management. In C. Kahraman and S. Çevik Onar (eds.), Intelligent techniques in engineering management: Theory and applications, Cham: Springer, pp. 221–245.

[10] **Jollivet, T., Peyrac, C. and Lefebvre, F.** 2013. Damage of composite materials. In 5th Fatigue Design Conference, Fatigue Design, Senlis, France.

[11] **Haojie, S., Yao, W. and Yitao, W.** 2014. Synergistic damage mechanic model for stiffness properties of early fatigue damage in composite laminates. Procedia Engineering, 74(2), pp. 199–209.

[12] **Kaminski, M., Laurin, F., Maire, J. F., Rakotoarisoa C. and Hémon, E.** 2015. Fatigue damage modeling of composite structures: The ONERA viewpoint. Journal AerospaceLab, 9(1), pp. 1–11.

[13] **Ali, S., Tahir, M. H., Saeed, M. A., Zaffar N. and Khan, M. K.** 2019. Design and development of fatigue machine: Rotating bending fatigue testing on different materials. International Journal of Advanced Engineering and Management, 4(2), pp. 8–15.

[14] **Mott, R. L., Vavrek E. M. and Wang, J.** 2018. Machine elements in mechanical design. New York: Pearson.

[15] **Nogueira, R. M., Meggiolaro, M. A. and Castro, J. T. P.** 2017. A fast rotating bending fatigue test machine. In 24th ABCM International Congress of Mechanical Engineering, Curitiba, Brazil.

[16] **Mirzaei, M., Karamoozian M. and Ghasemi, I.** 2019. Investigation on the mechanical properties of carbon fiber-reinforced polymer composite shafts under torsional loading. Journal of Composite Materials, 53(2), pp. 141–153.

[17] **Huang, F., Wang, Z., Adjallah K. H. and Sava, A.** 2020. Bearings degradation monitoring indicators based on discarded projected space information and piecewise linear representation. International Journal of Mechatronics and Automation, 7(1), pp. 23–31.

[18] **Basson, C. I., Bright, G., Padayachee, J. and Sarp, A.** 2023. Investigation of predictive maintenance algorithms for rotating shafts under various bending loads. In Smart, Sustainable Manufacturing in an Ever-Changing World: Proceedings of International Conference on Competitive Manufacturing (COMA'22). Cham: Springer, pp. 497–510.

[19] **Jolliffe, I. T. and Cadima, J.** 2016. Principal component analysis: A review and recent developments. Philosophical Transactions A, 374(2065), 20150202.

[20] **Tiddens, W., Braaksma, J. and Tinga, T.** 2020. Exploring predictive maintenance applications in industry. Journal of Quality in Maintenance Engineering, 28(1), pp. 68–85.